LARGE-APERTURE, HIGH-DAMAGE-THRESHOLD OPTICS FOR BEAMLET

J. H. Campbell   R. T. Maney

L. J. Atherton   R. C. Montesanti

J. J. DeYoreo   L. M. Sheehan

M. R. Kozlowski   C. E. Barker

Introduction

Beamlet serves as a test bed for the proposed National Ignition Facility (NIF) laser design and components. Therefore, its optics are similar in size and quality to those proposed for the NIF. In general, the optics in the main laser cavity and transport section of Beamlet are larger and have higher damage thresholds than the optics manufactured for any of our previous laser systems. In addition, the quality of the Beamlet optical materials is higher, leading to better wavefront quality, higher optical transmission, and lower-intensity modulation of the output laser beam than, for example, that typically achieved on Nova. In this article, we discuss the properties and characteristics of the large-aperture optics used on Beamlet.

The damage threshold is perhaps the most critical property of the optical materials, because the cost of the laser system is driven largely by the amount of laser energy that can be delivered in a given aperture size. The higher the transmitted energy density (fluence), the fewer the number of laser beams needed to meet the output energy requirement and, therefore, the lower the overall system cost. Consequently, Beamlet (and NIF) are designed to operate near the damage threshold limit for the optical materials.

Table 1 summarizes the damage threshold requirements at 1.0 and 0.35 μm for the large optics on Beamlet for a nominal operating pulse length of 3 ns and lists the measured damage thresholds for comparison. Note that the measured thresholds represent the absolute maximum operating laser fluence possible for that specific optic. To provide a safety margin for our designed operating limit, we multiply the measured thresholds by a "de-rating" factor that accounts for measurement uncertainties. The product of the measured damage threshold times the de-rating factor is called the "safe operating limit" and represents the fluence limit for that specific optic. Beamlet is designed to never exceed the safe operating limits.

Figure 1 compares the peak designed laser fluence at key optical materials on Beamlet with the safe operating threshold. These peak fluences are reached during the final pass through the laser and are based on model calculations. Note that the peak fluence

TABLE 1. Beamlet's damage threshold requirements and measured values at 3 ns for various optical materials.

	Optics	Measured damage threshold (J/cm^2)	Safe operating limit (J/cm^2)	Beamlet peak fluence (J/cm^2)
1ω	Laser glass	34	28	20
	HfO$_2$/SiO$_2$ HR	26	18	8
	HfO$_2$/SiO$_2$ polarizer	18	13	8
	SiO$_2$ sol-gel AR	34	29	21
	KDP doubler	43	30	20
	KDP (Pockels cell)	43	30	8
3ω	KD*P tripler	20	14	11
	SiO$_2$ sol-gel AR	19	16	11

HR=high reflectivity; AR=antireflection

determines the damage limit of the laser, whereas the average fluence determines the energy output. Therefore on the Beamlet, we have worked hard to keep the peak-to-mean intensity variation within the laser pulse as low as possible to maximize the energy out and to minimize the risk of optical damage. Because laser optical materials do not all have the same damage thresholds, one or two materials generally limit the performance of the system. In the case of Beamlet, the optical material at most risk is the HfO_2/SiO_2 multilayer thin film polarizer (at 1ω) and the deuterated potassium dihydrogen phosphate (KD*P) tripling crystal (at 3ω).

Optical Materials

The optical materials on Beamlet can be divided into four main types: laser glass, potassium dihydrogen phosphate (KDP)/KD*P, dielectric coatings, and lenses and diagnostic beam splitters. This section briefly describes each of these materials and their key properties.

Laser Glass

The energy storage medium for the Beamlet flash-lamp-pumped amplifiers is a commercial phosphate laser glass (composition LG-750) manufactured by Schott Glass Technologies Inc. It has an Nd^{3+} doping concentration of $3.4 \times 10^{20}/cm^3$ and consists of a meta-phosphate glass composition. Although the details of the composition are proprietary, it contains the major oxides P_2O_5, Al_2O_3, K_2O, BaO, Nd_2O_3, and a number of other miscellaneous components.

For Beamlet (and NIF) the laser glass is in the form of large rectangular plates $78.8 \times 44.8 \times 4$ cm^3 (Fig. 2). The volume of these glass plates or "slabs" is about 14 L. For comparison, the largest pieces of Nova laser glass are elliptically shaped disks and have a volume

of about 7 L. Thus, the size and shape of Beamlet's slabs required a significant advancement in the prior laser glass manufacturing process. A total of 20 slabs were manufactured for the Beamlet laser—16 are installed on the system, and 4 are reserved as spares.

The size of the Beamlet laser slabs is driven by four main factors: (1) The maximum beam size, which is 35 cm for Beamlet. In addition, the laser slab is mounted in the amplifier cavity at Brewster's angle, requiring that the slab be lengthened to account for both the angle and the refractive "walk-off" of the beam as it travels through the glass. (2) The vignetting effect, allowing for the beam to propagate back and forth four times through the main laser cavity slightly off-axis to pass through the four different pinholes. (See "System Description and Initial Performance Results for Beamlet," p. 1.) The contribution of the vignette to the slab size is dependent on the length of the cavity amplifier section, the focal length of the spatial filter lens, and the pinhole spacing. (3) The alignment allowance which, within the main laser cavity, is set at 2% of the maximum beam size. (4) The stand-off distance from the edge cladding, required to avoid wavefront distortion of the beam caused by amplified spontaneous emission (ASE) heating the cladding. When the cladding is heated, it expands and distorts the region near the edge of the slab. Based on experiments,[1] the stand-off distance from the edge cladding bond line needs to be at least $t/2$, where t is the slab thickness. Since Beamlet slabs are 4 cm thick, the minimum stand-off distance is 2 cm around the border of the entire slab.
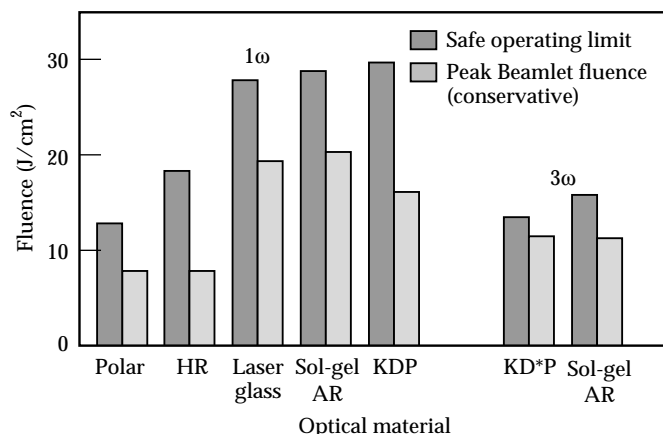
FIGURE 1. Comparison of the peak laser fluence during the final pass through the laser system with the "safe operating limits" of the material. The data are for a nominal square output pulse of 3 ns.
(70-50-0693-2242pb01)

FIGURE 2. Beamlet's $78.8 \times 44.8 \times 4$ cm^3 laser slab containing 3.4×10^{20} Nd^{3+}/cm^3; the edges of the laser slab are clad with a Cu:Doped phosphate glass designed to absorb ASE at 1054 nm.
(70-50-0393-0716pb01)

The laser slabs are clad with Cu:Doped phosphate glass having an absorption coefficient at 1.05 μm of 0.28/mm. The base composition of the cladding glass is the same as LG-750 (without the Nd^{3+}) and is bonded to the laser slabs using an epoxy adhesive specially formulated to match the index of the laser glass. Details for the cladding process are described elsewhere.[2] The laser slabs were clad and finished by Zygo Corporation and Eastman Kodak Company.

Laser glasses are specially formulated to give the desired laser, optical, thermal-mechanical, and physical-chemical properties needed for a specific application. Most of these properties are controlled by the base composition of the glass. However, some critical properties are also impacted by the manufacturing process. These include the optical absorption at 1054 nm, optical homogeneity, Nd^{3+} fluorescence lifetime, and the Pt inclusion content. Because of Beamlet's larger slabs, we were concerned whether these critical properties could be maintained throughout the process. Figure 3(a) shows the variation in optical absorption at 1054 nm for all the slabs produced. Optical absorption arises from either impurities in the raw materials and/or contaminants that enter during the processing (e.g., contaminants added by dissolution of the melter refractory walls).[3] The absorption offsets the laser gain of the material, thereby requiring either more amplifiers or harder pumping. The data in Fig. 3(a) show that the Beamlet slabs have very low absorption loss and meet the necessary absorption specification. In fact, about 30% of the absorption loss (i.e., 4.5×10^{-4} cm^{-1}) is due to absorption by the thermal population of Nd^{3+} in the lower laser level ($^4I_{11/2}$).

The Nd^{3+} fluorescence lifetime is mainly a function of the glass composition. To efficiently store energy in the amplifiers requires long fluorescence lifetimes. Two features of the manufacturing process can affect the lifetime—Nd^{3+} doping concentration and H_2O absorbed in the glass. The Nd^{3+} content affects the lifetime at high concentrations through the well-known concentration quenching mechanism.[4] Therefore, to avoid melt-to-melt variability in fluorescence lifetime, careful control of glass volatility during the melt cycle and precise addition of Nd^{3+} are necessary. Absorbed H_2O of only a few ppm can also affect the lifetime; therefore, very dry conditions must be maintained during melting. The hydroscopic nature of molten-phosphate laser glass makes it particularly vulnerable to H_2O uptake. The H_2O content of the laser glass is quantified by measuring the –OH absorption at 3300 nm; Fig. 3(b) shows the results from the Beamlet melt. Although there is some variability, all slabs are quite dry having H_2O absorptions between ≈ 0.2–0.6 cm^{-1} at 3.3 μm. This absorption corresponds to about 6–18 ppm of H_2O. Because of the good control of the Nd^{3+} doping concentration ($3.4 \pm 0.1 \times 10^{20}$/cm^3) and the H_2O content, all laser glass slabs exceed the Nd^{3+} fluorescence lifetime specification shown in Fig. 3(c). The Nd^{3+} lifetime specification for Beamlet laser glass is
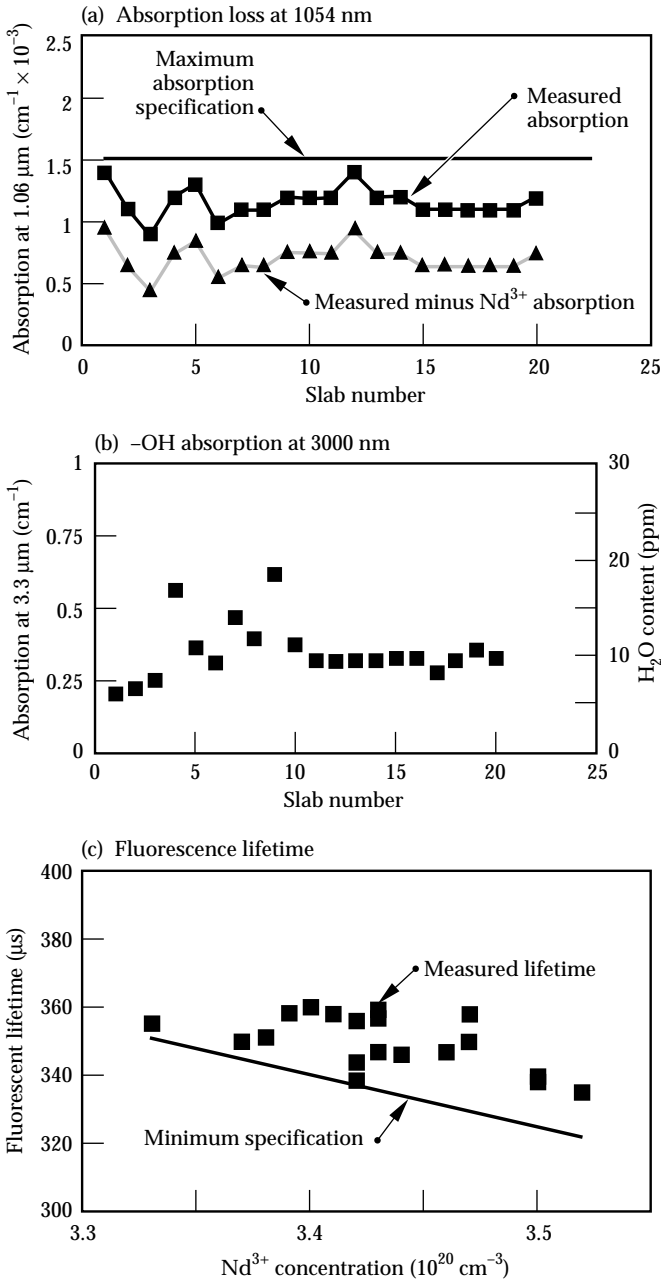

FIGURE 3. Summary of three key properties of the laser slabs produced for Beamlet compared with the design specifications: (a) absorption loss at 1054 nm, (b) –OH absorption at 3000 nm, and (c) fluorescence lifetime. The lifetime measurements were performed on samples $5 \times 5 \times 0.5$ cm^3.   (70-50-0295-0397pb01)

$$\tau_L \geq 340 - 150\left(\left[Nd^{3+}\right] - 3.4\right) \quad , \qquad (1)$$

where $[Nd^{3+}]$ is the Nd-ion concentration in units of $10^{20}/cm^3$ and τ_L is the minimum acceptable lifetime (in microseconds). In arriving at this specification, we also included the effects of radiation trapping by the $5.0 \times 5.0 \times 0.5 cm^3$ standard sample size used by vendors for routine fluorescence lifetime measurements. The specification also includes the effects of concentration quenching at high Nd-dopings, derived from work by Jancaitis.[5]

The Beamlet melts have very low residual H_2O content so there is little effect of –OH quenching on the lifetime. At low levels of H_2O contamination, the effect of –OH in reducing the lifetime can be estimated from the expression[6]

$$\Delta\tau = -7.62(\alpha_{3.3\,\mu m}) , \qquad (2)$$

where $\alpha_{3.3\,\mu m}$ is the measured –OH absorption at 3.3 μm and $\Delta\tau$ is the lifetime reduction relative to a sample with zero residual H_2O. For Beamlet's laser glass, the residual H_2O contributed less than a 4-μs reduction in lifetime.

We maintained good optical homogeneity during the manufacturing process with all the laser slabs meeting the homogeneity specifications. Because of the rectangular shape of the glass, there was some concern whether the homogeneity could be maintained in the corners of the slabs. All finished Beamlet laser slabs had <0.1 wave (at 1.054 μm) transmitted wavefront distortion across the clear aperture.

The damage threshold of the laser glass is controlled by the quality of the surface and the presence of absorbing impurities. The typical high-quality "super" polish used to finish laser glass gives a damage threshold in excess of 30 J/cm^2 at 3 ns (1054 nm) and, therefore, exceeds the requirements for Beamlet (Table 1). More important is the presence of absorbing particles within the glass, particularly Pt inclusions. Pt inclusions originate from the Pt containers used to melt the laser glass and can cause optical damage at fluences of 2–3 J/cm^2 at 3 ns, far below the Beamlet operating fluence. In addition, damage from large inclusions can grow with successive shots, eventually rendering the slab useless. Using new glass-melting processes,[7,8] we were able to maintain inclusion levels well below our manufacturing goal of <15 in any given slab and an average for all 20 Beamlet slabs of <3 inclusions per slab. In fact, 50% of the laser slabs had no inclusions at all and 90% had 3 or less.

KDP/KD*P

Large plates of single-crystal KDP are used in the Beamlet Pockels cell and frequency converter. The Pockels cell and second-harmonic generation crystals are undeuterated, whereas the harmonic tripling crystal is deuterated to a level of about 80%. (KD*P is the commonly used representation of the deuterated material.) The KDP and KD*P crystals are arguably the most difficult optics to manufacture and require the greatest production time. In addition, they represent a marked increase in size and quality over the crystals that were manufactured for Nova. For example, the crystal plates used on Beamlet are $37 \times 37 cm^2$ compared with $27 \times 27 cm^2$ on Nova. In addition, the Beamlet damage threshold requirement exceeds that required for Nova by about a factor of three.

The use of deuterated material for the third-harmonic crystal is driven by the need to suppress stimulated Raman scattering (SRS) at 3ω. At high drive intensities (such as those used on Beamlet) the spontaneous Raman-scattered light is amplified as it traverses the crystal face. The SRS gain coefficient in KDP has been measured to be approximately 0.23 cm/GW[9,10] at 3ω for a Type II tripling crystal. The scattered Raman Stokes intensity I_s grows as it travels a distance l across the crystal, according to the relationship

$$I_s(l) = I_s(0) \exp\left(gI_p l\right) \qquad (3)$$

where I_p is the pump intensity (GW/cm^2) and g is the gain coefficient. Because of the large aperture used on Beamlet, there is a significant gain-path length for the SRS light. Therefore, at high operating intensity (>3.0 GW/cm^2), the potential exists for the transversly propagating SRS light to reach intensities high enough to damage the KD*P.

The magnitude of the SRS gain coefficient for a particular Stokes Raman band is proportional to the scattering cross section. Therefore, because the spontaneous Raman band at 915 cm^{-1} is the most intense in KDP, it presents the greatest threat of unacceptable SRS. In KD*P, the mode at 915 cm^{-1} is split into two peaks and the magnitude of each band is dependent on the deuterium concentration (Fig. 4). At high deuteration levels, the Raman scattering cross sections for the two bands are about a factor of two lower than that for the single band of the undeuterated KDP. Therefore, deuterating the KDP greatly reduces the SRS threat to the tripling crystal.

The Beamlet crystal plates were cut from large single-crystal boules of KDP and KD*P, grown from aqueous solution by Cleveland Crystals, Inc. The KDP and KD*P boules produced for Beamlet weigh as much as 500 kg and take up to 2 years to grow (Fig. 5). This is about a factor of three increase in boule volume over those grown for Nova. The crystals required for the Pockels cell and harmonic converter system are
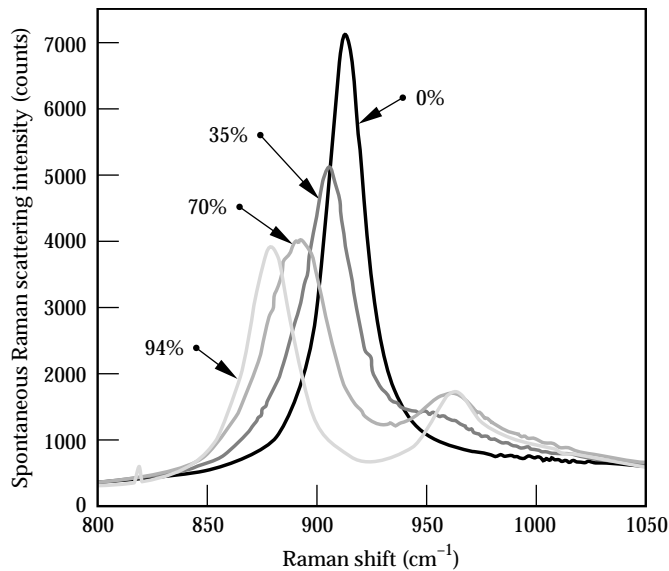
FIGURE 4. Measured spontaneous Raman scattering intensity profile for the 915 cm^{-1} mode at different deuteration levels. (70-35-0195-0316pb01)
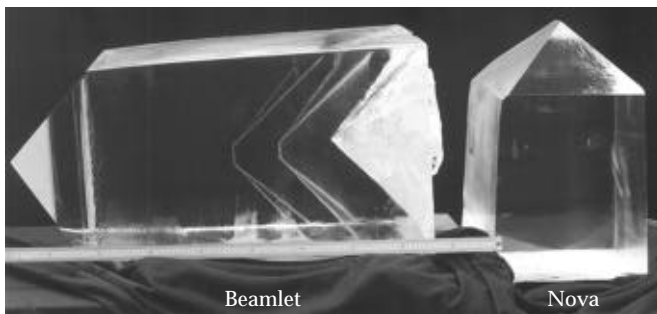

FIGURE 5. Photograph of a large KDP single crystal grown for Beamlet (note the meter stick shown for scale). The Beamlet crystals each weigh about 500 kg and are the largest ever produced. The smaller crystal on the right is the size grown for Nova. (70-39-1093-3487pb01)

then cut from these boules in an orientation shown schematically in Fig. 6. The Pockels cell uses a crystal cut normal to the *z*-axis of the boule, whereas the frequency-conversion crystals are cut at the phase matching angles required for the specific harmonic generation scheme. Beamlet uses a Type I/II third-harmonic generation method. (The harmonic generation system is described in detail elsewhere.[11])
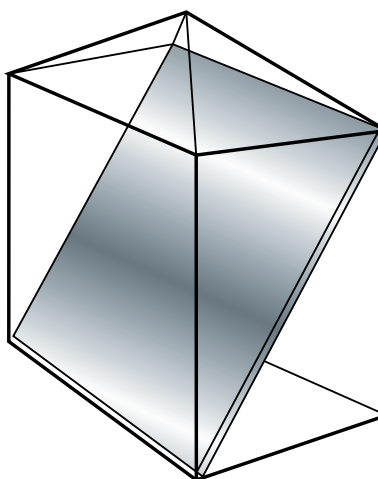
We chose to grow 80% deuterated material (vs 95%) because the level of stress-induced birefringence was expected to be lower and the time to grow the boules was expected to be shorter. Deuterated water (D$_2$O), having a deuteration level of 99.7%, was obtained from the Department of Energy's national stockpile. In general, the growth rate for fully deuterated material is as much as 10 times slower than for undeuterated KDP.

Apart from size and deuteration level, the quality of the KDP and KD*P crystals is also of critical importance. Specifically, stresses within the crystal can lead to stress-induced index variations and birefringence that in turn can produce distortions in the optical wavefront and beam depolarization.[12–14] Wavefront distortion and depolarization degrade the performance of the laser. For example, in the case of the Pockels cell, any depo-larization in the beam results in a direct transmission loss at the polarizer. Likewise, wavefront distortions can reduce the conversion efficiency of the harmonic generator, produce downstream modulation, and degrade focusability. Our operating goal for the Pockels cell was to produce <1% depolarization loss for any given pass and to keep the transmitted wave-front distortion and wavefront gradients for the finished crystal to <λ/4 and λ/4/cm, respectively.
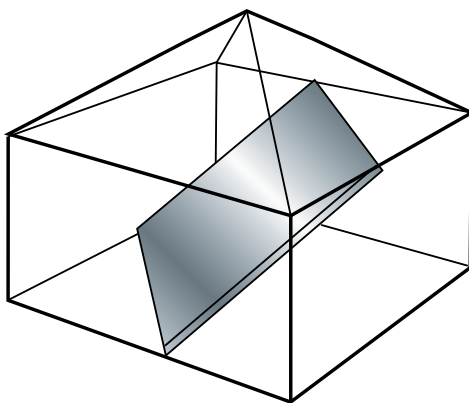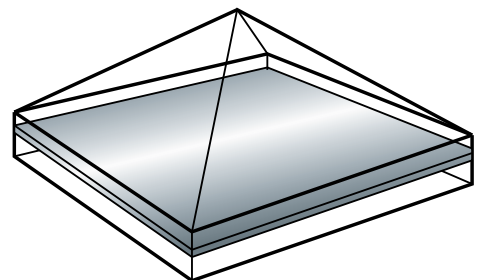

FIGURE 6. Schematic diagram showing the orientation in which the crystal plates used on Beamlet are cut from large KDP and KD*P single-crystal boules. (a) Type I doubler, (b) Type II tripler, and (c) Pockels cell *z*-plate. In general, several crystals of a given type can be cut from one boule. (70-35-0195-0317pb01)

The birefringence (δn) in a Pockels cell plate, cut normal to the z-axis of the crystal, is dominated by the shear strain and is given by[10]

$$\delta n = n^3 p_{66} \varepsilon_{xy},\tag{4}$$

where n is the refractive index, ε_{xy} is the shear strain, and p_{66} is the elasto-optic tensor element appropriate for this geometry; p_{66} has the value of 0.028 for KDP and 0.025 for K*DP. The depolarization loss (L), due to this birefringence, is given by[12]

$$L = \sin^2\left[\left(\frac{\pi}{\lambda}\right)\delta n t\right],\tag{5}$$

where t is the crystal thickness and λ is the laser wavelength. Equation (5) is valid for the "on" and "off" states of the Pockels cell (i.e., when the voltage applied across the crystal is either $V\pi$ or 0, respectively). The shear strain can be directly related to the shear stress, τ_{xy}:

$$\tau_{xy} = C_{66} \varepsilon_{xy},\tag{6}$$

where C_{66} is the elastic constant and has the value of 6.24 and 5.94 GPa for KDP and KD*P, respectively. To achieve a depolarization loss of 1% or less requires a shear stress $<10^6$ Pa.

Distortions in the beam phase front transmitted through the Pockels cell z-plate are controlled by the residual normal strains in the crystal:[12]

$$\Delta n = \left(\frac{n^3}{2}\right)\left[\frac{1}{2}\left(p_{11} + p_{12}\right)\left(\varepsilon_x + \varepsilon_y\right) + p_{13}\varepsilon_z\right],\tag{7}$$

where Δn is the index shift, the p_{ij}'s are elasto-optic coefficients, and ε_x, ε_y, and ε_z are the normal strains in the crystal. These strains can be related to residual normal stresses using the relationships developed by DeYoreo and Woods.[14] The index shift produces a spatial variation in the transmitted phase given by

$$\phi = \left(\frac{2\pi}{\lambda}\right)\Delta n t.\tag{8}$$

To meet the transmitted wavefront distortion specification of $<\lambda/4$ for the Pockels cell KDP crystal, requires a minimum residual normal stress field of $\approx 10^5$ Pa. Also, to meet the transmitted wavefront gradient specification for the crystal requires that the stress gradient be $<10^5$ Pa/cm.

The birefringence and wavefront distortions of the crystals used on Beamlet are characterized using the method described by DeYoreo and Woods.[13] Figure 7 presents the measured polarization efficiency (i.e., 100%—% depolarization loss) for a 32×32 cm^2

(a) Polarization efficiency—KD*P crystal
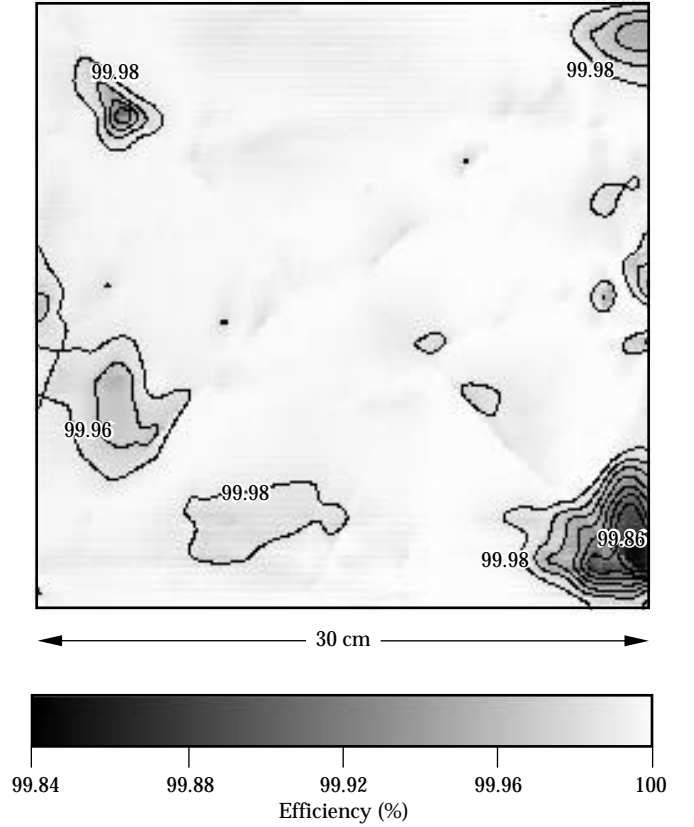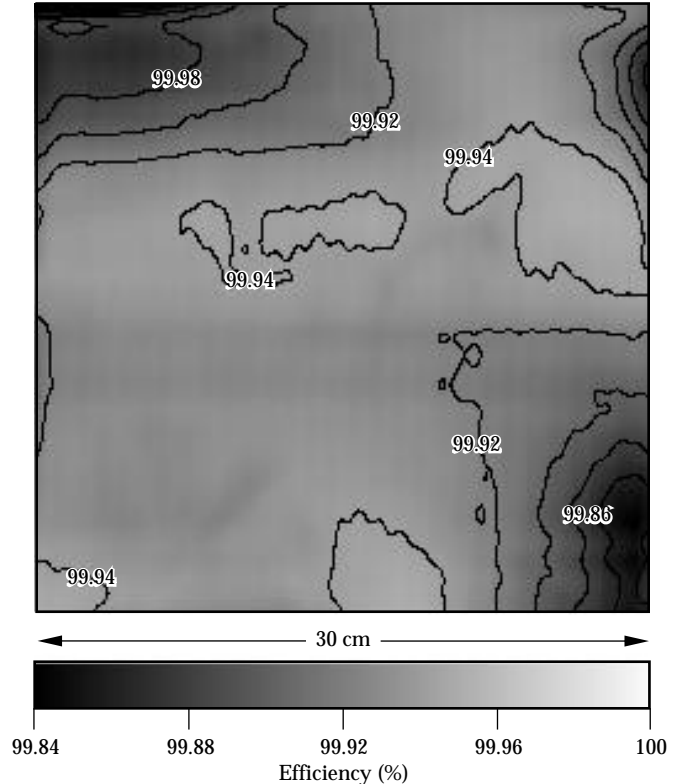

(b) Polarization efficiency—KDP crystal

FIGURE 7. Polarization efficiency of z-cut (a) KD*P and (b) KDP plates expressed as the percent of the output energy in the correct polarization state, i.e., 100%—% depolarization loss. The crystal plate dimensions are $32 \times 32 \times 1$ cm^3. (70-50-1294-3982pb02)

KDP crystal. The data show a maximum loss of 0.4% through any point in the crystal with an aperture loss averaging 0.05%. The data show that the maximum residual shear stress in the crystal is $<1.5 \times 10^5$ Pa. Similarly, interferometry measurements show phase-front distortions from the bulk material of less than an eighth of a wave at 1054 nm, again suggesting very low residual normal stresses in the crystal.

The KDP crystal plates are finished by diamond turning instead of polishing. In this process, a crystal blank is mounted on a carriage that translates the crystal blank parallel to the cutting plane. The cutting plane is defined by the single-point diamond tool mounted at a fixed radius in a high-speed spindle. This is commonly referred to as a fly-cutting mode of operation, and the cutting direction can be more closely aligned with a preferred axis on the crystal. By rotating the tool, rather than the crystal, the cutting rate remains the same across the whole face of the crystal. During the final finishing steps, the distance between subsequent tool cuts is usually only a few micrometers. Using this method, surface finishes of about 30 Å (rms) are typical.

One recurring problem we have encountered during finishing of large KDP crystals is a small-scale waviness in the transmitted wavefront. Our initial tests on Beamlet showed this same waviness in the output 1ω near-field image [Fig. 8(a)]. This waviness originated from the diamond-turned surface of the Pockels cell crystal and had a spatial scale length of about 6.3 mm. The measured amplitude of the phase ripple suggests a surface with a 100-Å peak-to-valley (p-V) periodic variation at that scale length. We investigated ways to reduce the surface waviness, because at high laser intensities the phase ripple from the diamond turning process may seed small-scale beam breakup due to self-focusing.[15] The source of the waviness was traced to a problem with the carriage system that translates the crystal. Specifically, we found that the flexure coupling that connects the drive-lead screw to the carriage was not properly aligned. Therefore, the flexure coupling was unable to adequately remove the natural once-per-revolution "wobble" motion of the lead screw. In this condition, the increased transmission of the lead-screw wobble into the carriage caused the crystal blank to move excessively in and out of the cutting plane in a sinusoidal fashion. After adjusting the flexure coupling, we found that the surface waviness was greatly reduced. Transmitted wavefront measurements on crystals finished before and after this repair showed that for scale lengths of ≈6 mm, the p-V surface waviness on the crystals was reduced from ≈60 Å to ≈10 Å above the background roughness near that spatial frequency. Figure 8 compares the near-field image of the Beamlet output beam before and after this corrective measure. Note that the circular arcs due to the spatial ripple are nearly absent in the "after" near-field image [Fig. 8(b)].

The damage threshold of some optical materials can be improved by "laser conditioning." KDP and KD*P are two such materials. During the process of laser conditioning, the optical material is exposed to a series of laser shots with monotonically increasing fluence. The wavelength of the conditioning laser shots is the same as the wavelength at which the optic is intended to be used. At the end of this sequence of exposures, the optical damage threshold is typically increased
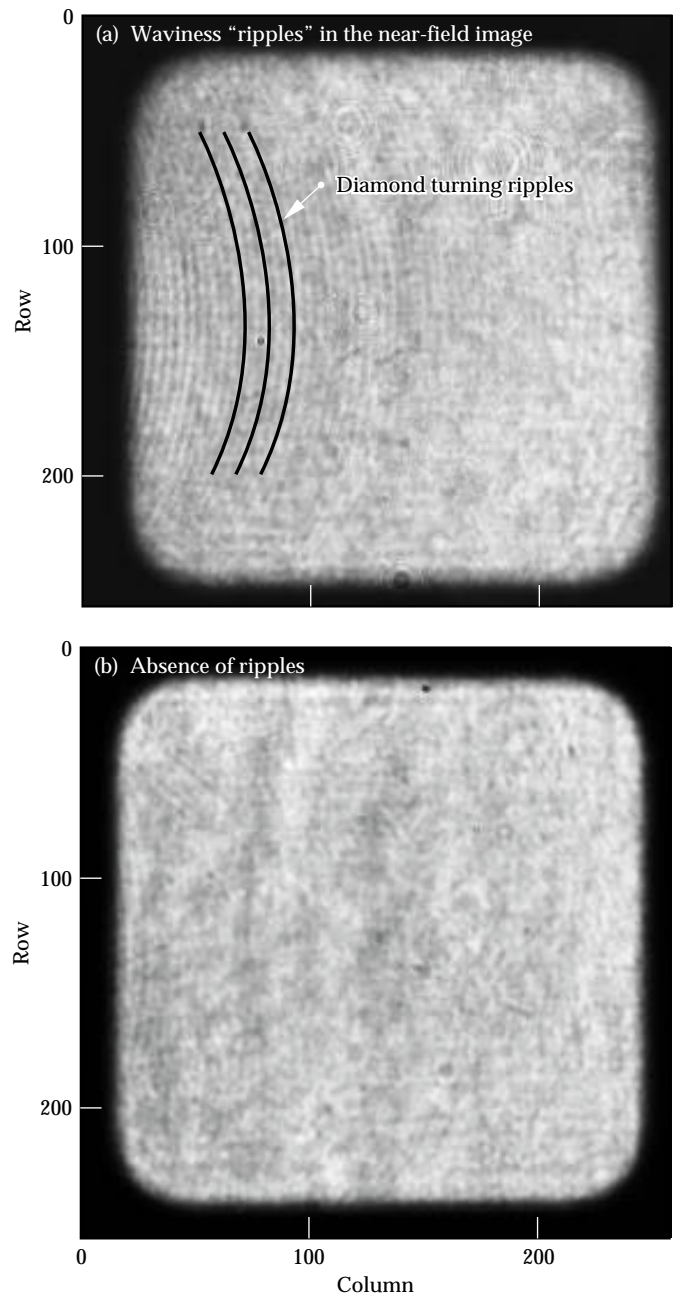

FIGURE 8. Near-field images of the 1ω output on Beamlet showing (a) the intensity modulation caused by diamond turning "ripples" on the Pockels cell KDP crystal, and (b) dramatic reduction of the ripples after the diamond turning machine is properly adjusted. (70-50-0295-0593pb01)

by a factor of two or more over the unconditioned (i.e., single-shot) threshold. As a general rule of thumb, at least five shots are needed to condition the optic to ≈85% of the maximum conditioned threshold. Furthermore, the first shot in the conditioning sequence should be at a fluence of about one-half the unconditioned damage threshold.

Table 2 summarizes the unconditioned and conditioned damage thresholds of KDP and KD*P at 1ω and 3ω, respectively.

Dielectric Coatings

Two main types of optical coatings are used on Beamlet: (1) multilayer HfO_2/SiO_2 high-reflectivity (HR) and polarizer coatings and (2) single-layer SiO_2 sol-gel antireflection (AR) coatings. Figure 9 shows the Beamlet polarizer and two of the mirrors. The sol-gel AR coating design, coating process, optical performance, and damage threshold have been well documented[16–18] and will not be discussed here. We note only that these coatings are routinely applied to all Beamlet and Nova transmissive optics (large and small) and have excellent transmission (>99.5% per surface) and high damage thresholds at 1ω and 3ω (Table 1).

Beamlet uses HfO_2/SiO_2 multilayer coatings because of their demonstrated damage threshold improvement with laser conditioning,[19,20] good optical properties, and relative ease in application over large apertures by electron beam (e-beam) evaporation.[21] All the multi-

layer coatings on large-aperture Beamlet optics were applied by conventional e-beam processing.

There are three reasons the polarizer is the most difficult optical coating to make: (1) The size of the polarizer is $75 \times 39 \times 9$ cm^3 and is more than twice the size of anything previously manufactured. (2) The damage threshold of the polarizer required for Beamlet represents a three-fold improvement over those used on Nova. (3) The coating layers need to be uniformly and precisely deposited over the entire substrate surface.

The polarizer coating was deposited on a BK-7 silicate glass substrate. BK-7 is significantly lower in cost than SiO_2, although it has the disadvantage of having a low bulk damage threshold due to Pt inclusions in the glass. However, because the polarizers used on Beamlet are used in reflection at high intensity, the BK-7 substrate is never exposed to damaging fluences.

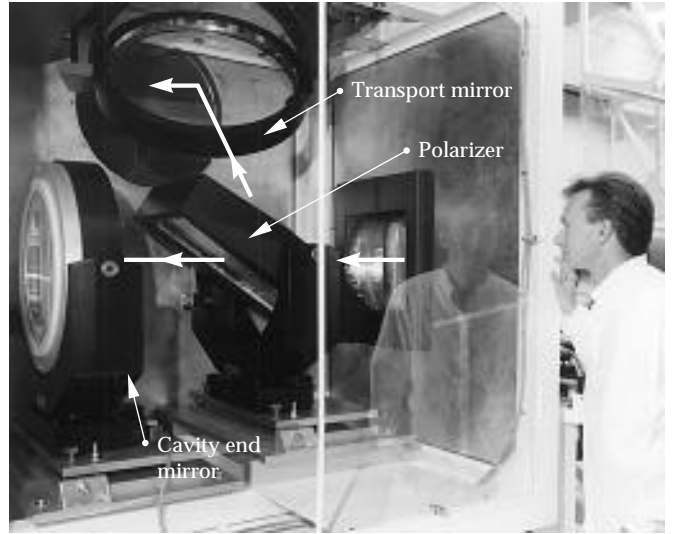Table 3 summarizes the transmission properties of the four polarizers manufactured for Beamlet by

FIGURE 9. Photograph of the large-aperture HfO_2/SiO_2 thin-film polarizer used with the PEPCs on Beamlet to switch the beam out of the multipass cavity. The polarizer is used in a transmissive mode at low fluence (p-polarized incident light) during the first and second pass. On the final pass, the light is s-polarized and reflected off the polarizer coating and out of the cavity. The peak fluence is about 11 J/cm^2 at 3 ns (1054 nm).   (70-50-0594-2486pb01)

TABLE 2. Summary of damage threshold for KDP and KD*P crystal plates used on Beamlet. The accuracy of the measurement is ±15% and ±30% for unconditioned and conditioned values.

Optic	Material	Wavelength (nm)	Damage threshold at 3 ns (J/cm^2)	
			Unconditioned	Conditioned
Pockels cell *z*-plate	KDP	1054	34	43
Type I doubler	KDP	1054	34	43
Type II tripler	KD*P	1054	16	25
		351	10	20

TABLE 3. Summary of transmission, extinction ratio, reflected wavefront distortion, and conditioned damage threshold for the four $79 \times 39 \times 9$ cm^3 HfO_2/SiO_2 thin film polarizers manufactured for Beamlet (measured in dry N$_2$). Damage threshold is accurate to ±30%.

Polarizer designation	Optimum use angle	Transmission (%) p-polarized T_p	Transmission (%) s-polarized T_s	Extinction ratio T_p/T_s	Reflected wavefront distortion (in waves at 1.05 μm)	Conditioned damage threshold at 1.054 μm and 3 ns (J/cm^2)[a] p-polarized	Conditioned damage threshold at 1.054 μm and 3 ns (J/cm^2)[a] s-polarized
1	55.5˚	98.2	0.60	163	0.4	18	23
2	54.5˚	98.1	0.10	981	0.25	20	26
3	56˚	98.0	0.25	392	0.28	13	18
4	54.5˚	98.2	0.14	701	0.38	20	35

[a]Damage measurements on witness samples from the production run.

Spectra-Physics. The optimum-use angle is between 54.5 and 56° and the polarizer can be "tuned" to the maximum extinction ratio by rotating the optical mount that holds the polarizer over the specified use range. We manufactured four polarizers: two are used on the system and two are spares. The polarizers were prepared in two separate coating production runs (with two polarizers in each run); the reproducibility between the two runs was quite good. Three of the polarizers had extinction coefficients >390, supporting the excellent control of the deposition process. The reflected wavefront distortion is between ≈0.25 and 0.4 waves and is largely due to spherical aberration that can be easily corrected by other optical elements in the system.

HfO_2/SiO_2 e-beam coatings can be laser conditioned to improve their damage threshold. (The conditioning process is similar to that described previously for KDP.) The conditioned damage thresholds of the polarizers all exceeded the Beamlet safe operating limit of 8 J/cm² at 3 ns (Table 3). The polarizers were conditioned off-line using the output from a pulsed Nd:YAG laser, operating at 10 Hz, to scan the full aperture of the optic in incremental fluence steps.[22] The conditioning effect has been associated with the gentle removal of nodular-shaped defects, which are known to limit the damage threshold of these multilayer coatings.[23] Based on measurements, the damage threshold of the polarizers scales with the pulse length as $\tau^{0.35}$.

The HfO_2/SiO_2 thin-film mirrors on Beamlet all had measured damage thresholds exceeding 25 J/cm² and reflectivities >99%. Damage thresholds of mirror coatings are typically higher than those of similar polarizer coatings.

Lenses and Diagnostic Beam Splitters

The lenses and diagnostic beam splitters used on Beamlet were all fabricated from fused silica, manufactured by Corning. The fused silica is prepared by flame-hydrolysis of $SiCl_4$ and is inclusion free. As a consequence, the damage threshold is limited by the surface finish and AR coating on the optic, not the bulk material. Extensive front-surface damage measurements at 1.0 and 0.35 µm and over a range of pulse lengths give a simple empirical relationship governing the safe operating limit for bare surface fused silica of

$$D = 22 \, t_p^{0.4} \text{ (at 1.0 µm)}$$

and

$$D = 9.2 \, t_p^{0.5} \text{ (at 0.35 µm)},$$

where t_p is the pulse length (ns) and D is the damage threshold (J/cm²). When a sol-gel AR coating is applied to the fused silica surface, the safe operating limit is slightly higher than that measured for the bare surface material, specifically[24]

$$D = 24.6 \, t_p^{0.4} \text{ (at 1.0 µm)}$$

and

$$D = 13.7 \, t_p^{0.5} \text{ (at 0.35 µm)}.$$

Summary

Nearly all of the large optics used on Beamlet represent a dramatic increase in size and optical quality over those used on previous ICF lasers. Specifically the laser slabs, KDP/KD*P crystals, and polarizers are more than a factor of two larger than those used on Nova. In addition, the damage thresholds and quality of the Beamlet optical materials are also improved by two- to three-fold over those used on Nova. The sizes and quality of optics used in Beamlet closely match those expected to be used in the proposed NIF.

Acknowledgment

UCRL-LR-105821-95-1

Notes and References

1. J. E. Murray, H. T. Powell, G .F. Ross, and J. D. Wintemute, Technical Digest, Annual Meeting, Opt Soc of Am, Washington, DC, TUU9 (1988).

2. J. H. Campbell, G. Edwards, F. Frick, D. Gemmell, et al., *Laser-Induced Damage in Optical Materials: 1986*, (NIST, Special Publication, Boulder, CO, 1987; *NIST* 752) p. 19.

3. S. E. Stokowski and D. Krashkevich, *Mat. Res. Soc. Symposium Proc.* 61, 273 (1986).

4. H. G. Danielmeyer, M. Blatte, and P. Balmer, *Appl. Phys.* 1, 269–274 (1973).

5. K. Jancaitis, "Updated Model for the Decay of the Inversion in LG-750 ND:Glass," LLNL internal memo, LS&T, 91–35 (Apr 1990).

6. J. A. Caird, N. D. Nielsen, and J. E. Murray, "Water Contamination and Fluorescence Lifetime in Nova Laser Glass," LLNL internal memo, ADG-88-138 (Dec 7, 1988).

7. J. H. Campbell, E. P. Wallerstein, J. S. Hayden, D. L. Sapak, et al., *Glastech. Ber. Glass Sci. Technol.* 68(1), 11–21 (1995).

8. J. H. Campbell, E. P. Wallerstein, H. Toratani, H. Meissner, et al., *Glastech. Ber. Glass Sci. Technol.* 68(2), 1–11 (1995).

9. R. A. Sacks, C. E. Barker, and R. B. Ehrlich, *ICF Quarterly Report* 2(4), 179–188, Lawrence Livermore National Laboratory, Livermore, CA, UCRL-LR-105821-92-4 (1992).

10. W. Lee Smith, F. P. Milanovich, and M. A. Henesian, LLNL memorandum UVM 83–02 (Feb. 25, 1983).

11. C. E. Barker, D. Milam, and R. Boyd, *ICF Quarterly Report* 3(2), 55–62, Lawrence Livermore National Laboratory, Livermore, CA, UCRL-LR-105821-93-2 (1993).

12. J. J. DeYoreo, J. Britten, R. Vital, K. Montgomery, et al., *ICF Quarterly Report* 3(3), 103–111, Lawrence Livermore National Laboratory, Livermore, CA, UCRL-LR-105821-93-3 (1993).

13. J. J. DeYoreo and B. W. Woods, *Inorganic Crystals for Optics, Electro-Optics and Frequency Conversion*, (SPIE—International Society for Optical Engineering, Bellingham, WA, 1991; *Proc. SPIE* 1561) p. 50.

14. J. J. DeYoreo and B. W. Woods, *J. Appl. Phys.* 73, 1 (1993).

15. J. T. Hunt, J. A. Glaze, W. W. Simmons, and P. Renard, *Appl. Opt.* 17, 2053–2057 (1978).

16. I. M. Thomas, *Appl. Opt.* 25, 1481 (1986).

17. I. M. Thomas, J. G. Wilder, W. H. Lowdermilk, and M. C. Staggs, *Laser Induced Damage in Optical Materials: 1984*, (NBS Special Publication, 1986; *NBS* 727) p. 205–210.

18. M. C. Staggs, D. Milam, I. M. Thomas, and J. G. Wilder, *Laser Induced Damage in Optical Materials: 1985*, (NBS Special Publication, 1988; *NBS* 746) p. 404–411.

19. M. R. Kozlowski, I. M. Thomas, J. H. Campbell, and F. Rainer, *Thin Films for Optical Systems*, (SPIE, Bellingham, WA, 1992; *Proc. SPIE* 1782) p. 105–121.

20. M. R. Kozlowski, C. R. Wolfe, M. Staggs, and J. H. Campbell, *Laser Induced Damage in Optical Materials: 1989*, H. Bennett, L. Chase, A. Guenther, B. Newnam, and M. J. Soileau, Eds., (NIST, Special Publication, 1990; *NIST* 801) p. 375.

21. M. R. Kozlowski, R. Chow, and I. M. Thomas, *Handbook of Laser Science and Technology*, M. Weber, Ed., (CRC Press, 1995) pp. 767–812.

22. L. Sheehan, M. Kozlowski, F. Rainer, and M. C. Staggs, *Laser Induced Damage in Optical Materials: 1993*, (SPIE, Bellingham, WA, 1994; *Proc. SPIE* 2114) pp. 559–568.

23. M. R. Kozlowski, R. J. Tench, R. Chow, and L. M. Sheehan, *Optical Interference Coatings*, (SPIE, Bellingham, WA, 1994; *Proc. SPIE* 2253) pp. 743–750.

24. J. H. Campbell and F. Rainer, Lawrence Livermore National Laboratory, Livermore, CA, Report, UCRL-JC-109255, *SPIE '92 Conference Proceedings*, San Diego, CA, July 1992.

25. Cleveland Crystals, Inc., 676 Alpha Dr., Highland Heights, OH 44143.

26. Corning Glass Works, MP-21-04-2, Corning, NY 14831.

27. Eastman Kodak Company, Dept. 177, Bldg. 601, Rochester, NY 14650–0803.

28. Schott Glass Technologies Inc., 400 York Ave., Duryea, PA 18642.

29. Spectra-Physics Components & Accessories, 1330 West Middlefield Rd., Mountain View, CA 94039–0517.

30. Tinsley Laboratories, Inc., 3900 Lakeside Dr., Richmond, CA 94806.

31. Zygo Corporation, Laurel Brook Rd., Middlefield, CT, 06455–0448.